



## OPEN ACCESS

EDITED BY  
Chenxi Li,  
Tianjin University, China

REVIEWED BY  
Hui Yu,  
Tianjin University, China  
Xiaochuan Dai,  
Tsinghua University, China  
Shuhua Yue,  
Beihang University, China

\*CORRESPONDENCE  
Xin Li,  
✉ cinlysmart@126.com

<sup>†</sup>These authors have contributed equally to this work

SPECIALTY SECTION  
This article was submitted to  
Optics and Photonics,  
a section of the journal  
Frontiers in Physics

RECEIVED 28 December 2022  
ACCEPTED 31 January 2023  
PUBLISHED 10 February 2023

CITATION  
Ding Y, Wei H, Liu X, Xu M, Sun D, Li T and  
Li X (2023), Rapid en-bloc hematoxylin-  
eosin staining for human lung cancer  
tissue for fluorescence micro-optical  
sectioning tomography.  
*Front. Phys.* 11:1132826.  
doi: 10.3389/fphy.2023.1132826

COPYRIGHT  
© 2023 Ding, Wei, Liu, Xu, Sun, Li and Li.  
This is an open-access article distributed  
under the terms of the [Creative Commons  
Attribution License \(CC BY\)](https://creativecommons.org/licenses/by/4.0/). The use,  
distribution or reproduction in other  
forums is permitted, provided the original  
author(s) and the copyright owner(s) are  
credited and that the original publication in  
this journal is cited, in accordance with  
accepted academic practice. No use,  
distribution or reproduction is permitted  
which does not comply with these terms.

# Rapid en-bloc hematoxylin-eosin staining for human lung cancer tissue for fluorescence micro-optical sectioning tomography

Yun Ding<sup>1†</sup>, Huaye Wei<sup>2†</sup>, Xin Liu<sup>1</sup>, Meilin Xu<sup>2</sup>, Daqiang Sun<sup>1,3</sup>, Ting Li<sup>4</sup> and Xin Li<sup>3\*</sup>

<sup>1</sup>Clinical School of Thoracic, Tianjin Medical University, Tianjin, China, <sup>2</sup>Department of Pathology, Tianjin Chest Hospital (Affiliated Hospital of Tianjin University), Tianjin, China, <sup>3</sup>Department of Thoracic Surgery, Tianjin Chest Hospital (Affiliated Hospital of Tianjin University), Tianjin, China, <sup>4</sup>Institute of Biomedical Engineering, Chinese Academy of Medical Sciences and Peking Union Medical College, Tianjin, China

**Objective:** To establish a rapid and effective method for en-bloc hematoxylin-eosin (HE) staining and paraffin embedding of human lung cancer and paracancerous tissues which can be applied to fluorescence micro-optical sectioning tomography (fMOST).

**Methods:** Human lung cancer and paracancerous tissues with a size of about 1 cm × 1 cm × 0.3 cm were taken and fixed in 10% neutral formalin. HE staining was performed using a heat water bath to facilitate staining. After staining, isopropyl alcohol was used for dehydration and transparency. Then, 65°C paraffin was used for wax immersion followed by paraffin embedding, while continuous paraffin sections were produced for observation.

**Results:** The tissues stained by en-bloc HE, dehydrated, transparent and wax immersion were slightly smaller in appearance, darker in color and slightly harder in texture than before. After paraffin embedding, the wax blocks did not show any obvious fragmentation, wrinkling or cavity formation, and could be continuously cut into 4- $\mu$ m thick slices which could be dragged to form wax tapes. The sections could develop flat in waterbath, and the tissues showed no signs of collapse or separation from the paraffin. After sections were picked up and dewaxed, the tissue structure was intact and the cell structure was clear under light microscopy, which could be used to evaluate the pathological features of lung cancer and paracancerous tissues.

**Conclusion:** We propose a suitable en-bloc HE staining of centimeter-sized lung cancer and paracancerous tissues that can be applied to fMOST. It is promising to be used in the accurate identification of structural landmarks and spatial assessment of lung cancer.

## KEYWORDS

en-bloc HE staining, paraffin embedding, lung cancer, histology, fluorescence micro-optical sectioning tomography

## Introduction

Lung cancer is a common malignancy worldwide and one of the leading causes of cancer deaths [1]. The pathology of lung cancer is obviously heterogeneous and closely related to the treatment and prognosis of patients. For example, the proportion of high-grade pathological subtypes is associated with the prognosis of patients with lung adenocarcinoma [2], and glandular structure is associated with tumor necrosis and lymphatic vascular invasion [3]. Currently, pathological section is still the gold standard for clinical diagnosis of lung cancer, which belongs to two dimensional (2D) spatial assessment. However, the reproducibility of histological structure assessment of lung adenocarcinoma by multiple pathologists is still a challenge [4]. In the study by Moreira AL et al. [5], the average Kappa value was  $0.84 \pm 0.04$  and the range of the Kappa value evaluating the grading agreement between the two observation groups (a total of 10 pathologists, 23 cases) was 0.79–0.89. Most of the inconsistent attributed to the distinction between the lepidic and papillary structures, as well as variations in the proportion of high-grade structures. Thus, the understanding of the main histological structure of lung cancer can improve the repeatability of lung cancer grading and classification among pathologists, which may ultimately lead to more accurate patient diagnosis, treatment, and prognosis guidance in the future [5].

Considering the limitations of traditional 2D images, Memorial Sloan Kettering Cancer Center [6] adopted Whole Slide Imaging (WSI) technology for 3D reconstruction of lung cancer. The WSI-based 3D imaging system has been used to recognize the existence of “tumor islands” in lung cancer, which in hindsight reflects an early identification of tumor spread through air spaces (STAS) that was reported to be associated with a higher recurrence rate and worse survival [7–9]. This emphasizes the clinical significance of 3D imaging because clinical therapy decisions are dependent on tumor development patterns (Gleason score). Good alignment, geometric congruence, and staining consistency are fundamental elements for a reliable 3D display [10]. Due to the variable staining intensities, paraffin sections are prone to distortion, shrinkage, folding, and color changes that may affect the accuracy and dependability of the reconstructed pictures [11]. In addition, it couldn't be utilized for physical images, such those taken with a light microscope. To get a non-destructive 3D image of lung cancer tissue, fMOST combined with propidium iodide (PI) staining were previously used to obtain the 3D imaging of the human lung adenocarcinoma tissues at single-cell resolution, and the bronchi and cells were reconstructed and visualized. However, PI staining shows no difference in all nuclei, so it is impossible to distinguish and track various cells in lung tissues according to the color results. Therefore, to identify the characteristic cells in lung tissues, it is necessary to explore new and appropriate overall staining methods of lung tissue blocks.

HE staining is the most commonly used staining method in clinical practice, and is essential for identifying the pathological characteristics of lung cancer, such as pathological subtypes, vascular invasion, and STAS. However, establishing a rapid en-bloc HE staining dehydration and paraffin embedding method that allows continuous sectioning is a great challenge. There are a few previous literatures on HE staining for whole tissue block, but the process of staining, dehydration, and paraffin embedding were laborious and time-consuming [12, 13]. In this study, we developed a simple, rapid, and reliable protocol for en-bloc HE staining, dehydration, and

paraffin embedding, which can be applied to serial sectioning, fMOST and 3D reconstruction for centimeter-sized lung cancer and paracancerous tissues for the first time.

## Materials and methods

### Samples and reagents

The surgically resected lung cancer and paracancerous tissue samples were obtained from 30 patients who underwent lobectomy in Tianjin Chest Hospital from August to September 2022.

The tissue fixation solution was 10% neutral formalin (Tianjin Jiusheng Medical Treatment Instrument Co., Ltd, Tianjin, China). Hematoxylin (Harris, BA4041, BaSO Biotech Co, Zhuhai, China) and eosin (water soluble, BA4024, BaSO Biotech Co., Ltd., Zhuhai, China) were selected for HE staining. Isopropyl alcohol ( $\geq 99.7\%$ , Xilong Scientific Co., Ltd., Guangdong, China) was used for dehydration and transparency. Paraffin wax ( $60^{\circ}\text{C}$ – $62^{\circ}\text{C}$ , Shanghai Huayong Olefin Co., Ltd, Shanghai, China) was used to embed the tissues and then sectioned. The study was approved by the Ethics Review Committee of Tianjin Chest Hospital (2022LW-024) and informed consents were taken from the patients.

### Sample collection and fixation

Lung cancer and paracancerous tissues with an approximate size of  $1\text{ cm} \times 1\text{ cm} \times 0.3\text{ cm}$  were taken and fixed in 10% neutral formalin for 24 h.

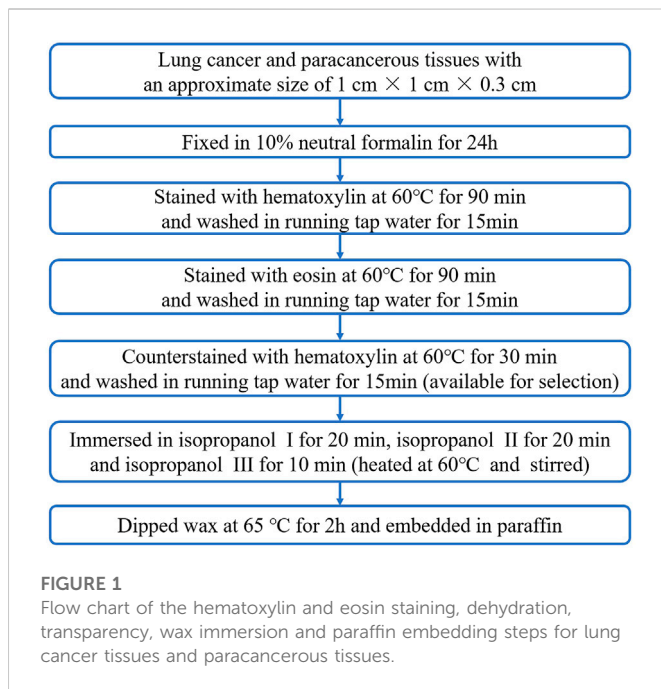
### En-bloc HE staining

The tissues were immersed in hematoxylin staining solution, stained in a water bath at  $60^{\circ}\text{C}$  for 90 min, and then washed in running tap water for 15 min. Next, the tissues were immersed in eosin staining solution, stained in a water bath at  $60^{\circ}\text{C}$  for 90 min, and washed in running tap water for 15 min. In addition, for those who prefer a bluer HE staining result, the tissues could be counterstained with hematoxylin (blue color), that is, the tissues were re-immersed in hematoxylin, stained in a water bath at  $60^{\circ}\text{C}$  for 30 min, and washed in running tap water for 15 min. While, for those who are accustomed to redder staining results, the hematoxylin counterstain time could be shortened, even not to carry it out.

Propidium iodide is a typical fluorescent nucleic acid dye that is frequently used to label DNA and RNA and distinguish normal cells from tumor cells by analyzing the cell karyotypes, making it the perfect way to observe all cells in a tissue or even a large organ during fluorescence imaging. In addition, PI staining adopts the technique of imaging while sectioning, avoiding the problem of imaging inhomogeneity, which is the most typical problem in the process of tissue staining. Thus PI staining was adopted in our previous study.

### Dehydration and embedding

After staining, the tissues were immersed in isopropyl alcohol I for 20 min, isopropyl alcohol II for 20 min, and isopropyl alcohol III for



10 min for dehydration and transparency. Each step was performed using water-bath shaking method at 60°C. After dehydration and transparency, the tissues were put into paraffin wax at 65°C for 2 h and then embedded with paraffin.

## Consecutive sectioning

The embedded paraffin tissue blocks were serially sectioned at a thickness of 4 μm with a microtome (Leica). The paraffin sections were placed into 45°C–48°C water, developed flat, and then picked up with a slide. The sections were heated in an oven at 75°C for 20 min and then deparaffinized in xylene I for 3 min and xylene II for 3 min. Finally, the sections were dripped with neutral resin and sealed with a cover slip. A schematic diagram of the procedure is shown in Figure 1.

## fMOST imaging with PI staining

Lung tissue imaging was performed on f-MOST system (Institute of Biomedical Engineering, Chinese Academy of Medical Sciences and Peking Union Medical College). The prepared-sample was submerged in a solution of PI and 0.01 M Na<sub>2</sub>CO<sub>3</sub> to provide a matching refractive index for the objective lens during imaging. Since the specimen was fixed on a precise three-dimensional translation platform for simultaneous dyeing, slicing and imaging, and a sample obtained at one time is called 1 strip. At the initial tool point, the specimen was driven by the 3D translation platform to produce the first cut along the positive X axis direction, and after the first strip is obtained, it returns to the initial tool point along the negative direction of the X axis, moves to the second tool point along the positive direction of the Y axis for the second tool cutting, and so on. Until the cutting of the whole layer of the specimen surface is completed, all the sample strips of this layer are obtained. At the same

time, the data were collected to obtain a cross-section imaging data of the tissue. Then, the 3D translation platform lifted the specimen with the thickness of the specimen slice, and cut the next layer according to the cutting strategy of the first layer until the slice imaging of the whole sample was completed.

## Results

### Tissue and wax block appearance

After determining the procedure, we performed en-bloc HE staining on 30 pairs lung cancer and paracancerous tissues in total, and achieved stable and good results, which were as follows. The lung cancer tissues were hard in texture without obvious shrinkage and fragmentation after en-bloc HE staining, dehydration, transparency and wax immersion (Figure 2A). The tissue was well fused with wax after paraffin embedding, and the surface of the wax block was flat, without cracks and bubbles. After the deep sectioning of the wax blocks (Figures 2B,C), there was no cracking of paraffin around the tissue, and the hardness of the tissue was uniform and good. The tissue cut surface was flat, and there were no obvious cracks, bubbles and breakage inside.

### Consecutive sectioning

The tissue was tough and tightly bounded to paraffin, and could be serially sliced at a thickness of 4 μm. The slices had no visible cracks or folds and could be dragged to form wax tapes (Figure 3A). The slices could develop flat in a water bath at 45°C–48°C, and the tissue did not spread and separate from the wax. It also worked well for solid lung cancer tissue. The continuous sectioning wax tapes of en-bloc HE stained and paraffin-embedded lung cancer and paracancerous tissues are shown in Figures 3B,C respectively.

### Scanning of slices

As shown in Figure 4, the microscopic structures of lung cancer and paracancerous tissues were kept in normal good shape without obvious atrophy and wrinkling, and the free cells, such as macrophages and tumor cells, in the alveolar spaces were clearly shown. At the same time, the cell structure was clear, and the nuclei and cytosol were distinctly colored, which were easy to observe microscopically. The staining of the tissue between adjacent sections was uniform, and the staining of the lung cancer with lower density and the paracancerous tissue were uniform in the same section, while some solid lung malignancies had lighter staining in the middle of a single slice. Furthermore, it showed that the accuracy of the sections made by staining-then-sectioning method was good for identifying the pathological characteristics of lung cancer. As seen in Figure 4A, pulmonary septum was widening, and pulmonary interstitial was fibrosis in lung cancer. Lung cancer cells grew adherent with the alveolar wall, obvious atypia of cancer cells were observed. While in paracancerous tissue (Figure 4B), phagocytic cells were found in alveolar cavity, and type I alveolar epithelial cells shown no obvious atypia.

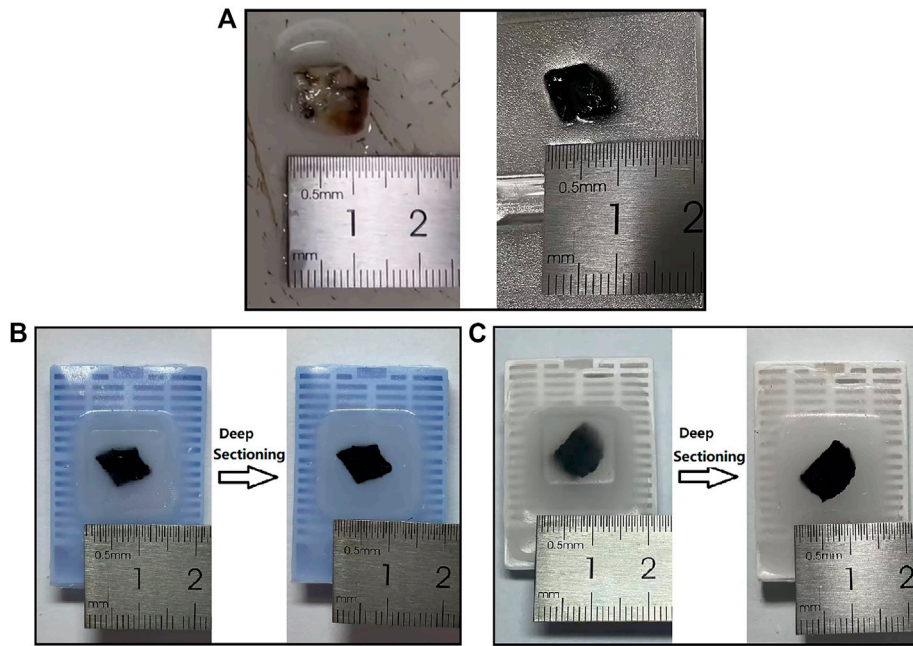


**FIGURE 2**

Tissue and wax block appearance. (A) Appearance of lung cancer tissue (left) and that after en-bloc HE staining, dehydration, transparency, and wax immersion (right). (B–C) Appearance of wax blocks after en-bloc HE staining and paraffin embedding (left) and deep sectioning (right) of lung cancer tissue (B) and paracancerous tissue (C). HE: hematoxylin and eosin.

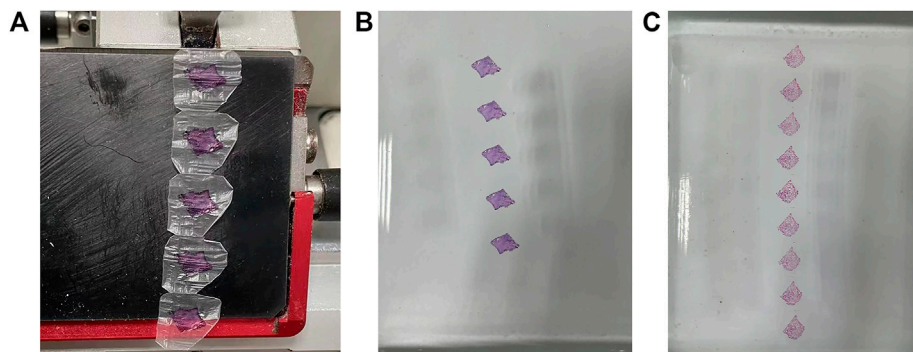


**FIGURE 3**

Wax tapes appearance. (A–B) Wax tapes of lung cancer tissue obtained by consecutive sectioning (A) were developed flat in a water bath at 45°C–48°C (B). (C) Wax tapes of paracancerous tissue were developed flat in a water bath at 45°C–48°C.

As shown in Figure 5, fMOST system combined with PI-staining were previously used to obtain the 3D imaging of the human lung adenocarcinoma tissues at single-cell resolution. Compared with paracancerous tissues, more solid components, more clustered cancer cells with larger nucleoli and more significant atypia were discovered in cancer tissues (Figure 5B). In the paracancerous tissue, the cancer cells grew along the original alveolar wall, mostly monolayer, few fibrous structures were observed. Alveolar epithelial cells in the paracancerous tissues formed acinar nets, which were scattered and had large voids, becoming alveoli (Figure 5A).

### 3D imaging

3D reconstruction imaging can be performed with both the staining-then-sectioning and sectioning-then-staining methods, the schematic diagram was shown in Figure 6 and the differences between these two methods for 3D reconstruction were summarized in Table 1. The staining-then-sectioning method can be applied to the fMOST technology, which can be used to *in-situ* imaging while sectioning, saving steps and time. At the same time, the 3D imaging based on the staining-then-sectioning method can effectively identify the pathological structure of lung cancer, such as pathological subtypes and STAS.

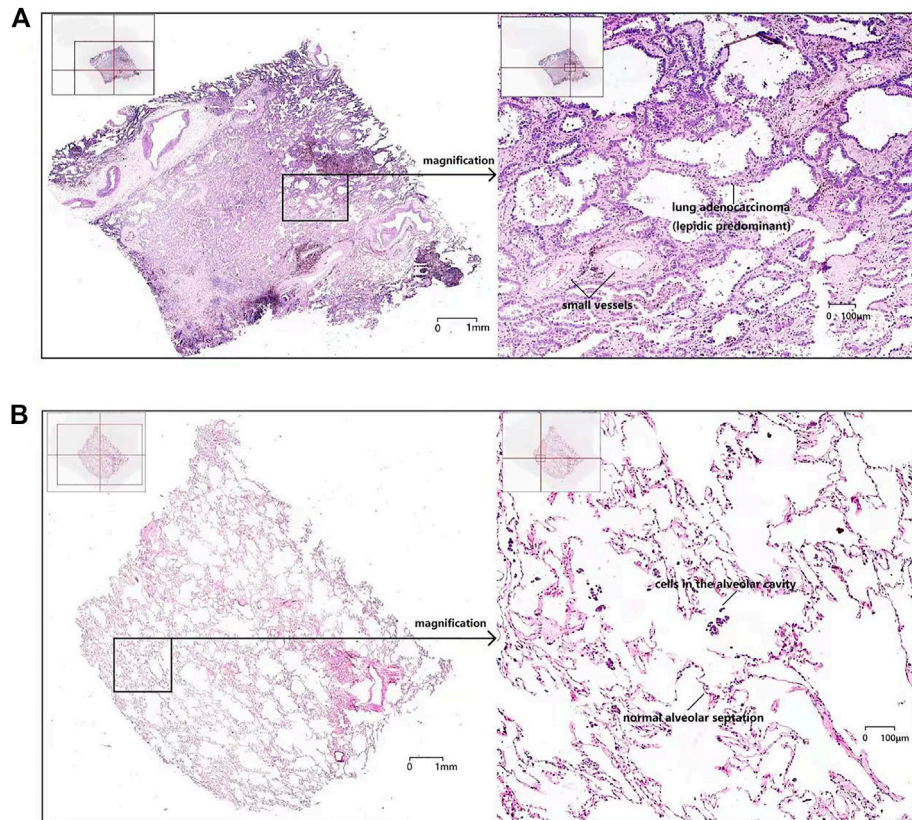


**FIGURE 4**

The scanning of an entire histologic slide (left, x20) and local magnification (right, x200) of a single section of lung cancer tissue (A) and paracancerous tissue (B).

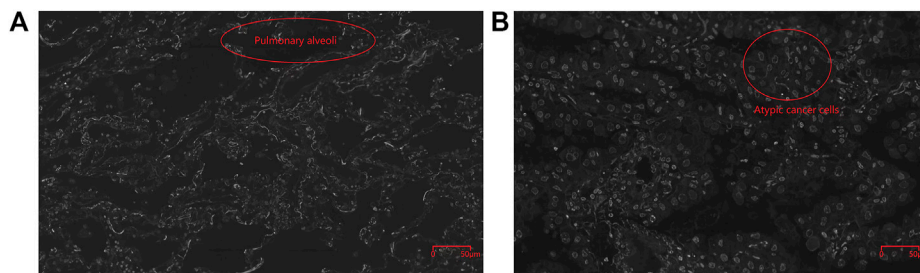


**FIGURE 5**

Cellular structure of cancerous (B, 400X) and paracancerous tissues (A, 400X) obtained by fMOST system combined with PI-staining with the spatial resolution of  $0.32 \times 0.32 \times 1.0 \mu\text{m}^3$ . Pulmonary alveoli was circled in red in Figure 5A and atypical cancer cells were marked by red circle in Figure 5B.

## Discussion

Recently, with the development of new techniques, the 3D visualization of pathological features of organisms have been gradually improved. For example, the fMOST technique has significantly improved misalignment in reconstruction by *in situ* micro-optical sectioning of the tissue block followed by 3D reconstruction [14]. 3D reconstruction of human lung tissue at the single-cell resolution can assist clinicians to study the detailed cellular

morphology, the anatomical relationship between cells, cell biology and function, so as to help clinicians in making more accurate assessments for the pathological characteristics of the lesion to guide the precision treatment of patients [15, 16]. However, these high-resolution 3D spatial imaging methods require en-bloc staining of lung cancer and paracancerous tissues. In our previously study, we attempted to obtain a complete 3D reconstruction of a lung adenocarcinoma at single-cell resolution using fMOST combined with PI staining, and the actual distribution of bronchi, respiratory

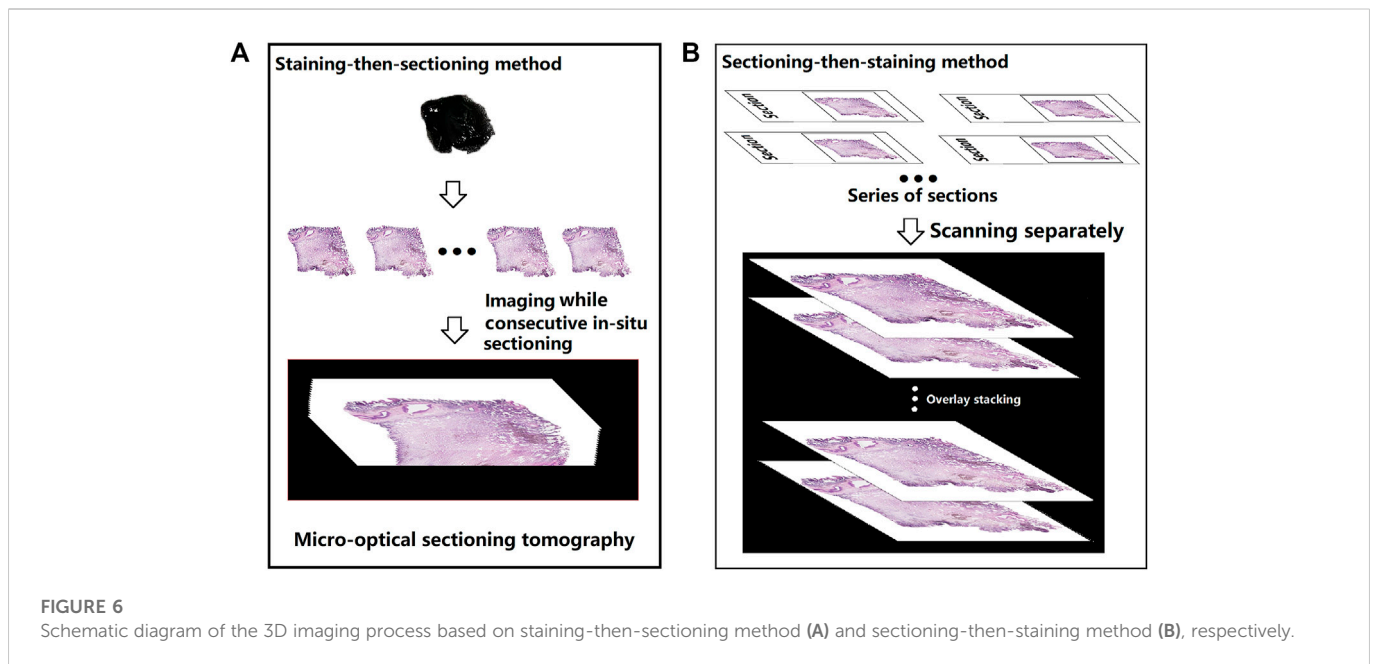


**FIGURE 6** Schematic diagram of the 3D imaging process based on staining-then-sectioning method (A) and sectioning-then-staining method (B), respectively.

**TABLE 1** The differences between the staining-then-sectioning method and the sectioning-then-staining method for 3D reconstruction imaging.

Contents	Staining-then-sectioning method for 3D imaging	Sectioning-then-staining method for 3D imaging
HE staining method	En-bloc staining at once	Staining for hundreds of sections separately
Color of adjacent layers	Almost no chromatic aberration	Slight chromatic aberration
Color of the same layer	Center of solid nodule is slightly lighter than periphery	Uniform staining
3D imaging method	<i>In situ</i> imaging while sectioning automatically	Overlay stacking imaging manually
Alignment between layers of 3D imaging	Good alignment between layers	Suboptimal alignment between layers
Overall process and time consuming	Comparatively fewer steps and time saving (approximately 5 h after fixation)	Comparatively more steps and time consuming (approximately 20 h after fixation)

3D: three dimensional; HE: hematoxylin-eosin.

bronchioles, terminal bronchioles, alveoli, and alveolar sacs were observed in accordance with the morphology disparities among various bronchus. Therefore, 3D reconstruction based on fMOST can be more tridimensional, more real, clearer and more intuitive to show the detailed information and location of the lesion [15, 16]. However, PI staining shows no difference in all nuclei, so it is impossible to distinguish and track various cells in lung tissue. HE staining is currently the most widely used method in the pathological diagnosis of lung cancer, nevertheless, it is difficult to establish rapid en-bloc HE staining and accomplish sequential sectioning after dehydration without fading. In this study, we overcame some of the previous difficulties in eb-bloc staining and after careful exploration, we developed a method for rapid en-bloc HE staining and paraffin embedding of centimeter-sized lung cancer and paracancerous tissues, which has a certain strengths, but there is still potential for improvement.

The following challenges need to be solved during the en-bloc HE staining and paraffin embedding. First, in order to stain the tissue as a whole quickly and evenly, the 60°C water bath method was used to

promote staining. Meanwhile, the peripheral tissue can avoid deep staining by being rinsed with running tap water after staining, which also makes the staining color in the same section as appropriate and uniform as possible. The rinsing with alkaline running tap water can also help to return to blue. In addition, there is no significant color difference between adjacent sections of the staining-then-sectioning method compared to the sectioning-then-staining method. Second, dehydration after en-bloc HE staining tends to cause fading. To solve this problem, water soluble HE staining solution was used for staining and isopropyl alcohol was chosen for rapid dehydration. Isopropyl alcohol can be employed as a dehydrating agent because it dissolves in water easily [17], and it does not dissolve in HE staining solution, the en-bloc stained tissue won't fade as a result of dehydration. Besides, there is little tissue shrinkage and little tissue sclerosis after isopropyl alcohol dehydration [18]. Furthermore, in order to avoid tissue contraction caused by the dehydration with anhydrous ethanol followed by isopropyl alcohol, this experiment was designed to omit anhydrous ethanol for dehydration. In addition to being a dehydrating agent, isopropyl alcohol can be employed as a

transparent agent and can substitute xylene to streamline processes, lessen tissue fading [19, 20], and facilitate wax immersion [18]. Third, it's difficult to complete dehydration because lung tissue contains a lot of gas, and the tissue in wax block is prone to contain air bubbles [21], thus leading to the formation of cavities in the sections and affecting the 3D reconstruction. Therefore, the tissues were put in an isopropyl alcohol bath at 60°C with shaking for dehydration, and wax immersion was taken at 65°C with higher melting point hard wax (60°C–62°C), as the gas in tissue was easier to discharge in high temperature [22, 23]. The gas can also be discharged by gently squeezing with forceps intermittently during dehydration and wax immersion, which does not damage the tissue structure. Moreover, dehydration was attempted to performed under negative pressure conditions ( $1.33 \times 10^4$  Pa) with heating, but there was no discernible benefit for dehydration or wax immersion. However, negative pressure dehydration can be performed for larger-sized lung tissues from interstitial lung disease patients [24].

In this study, we obtained a suitable scheme for the en-bloc HE staining and paraffin embedding of centimeter-sized lung cancer and paracancerous tissues by groping effective methods and verifying repeatedly. This method can be mainly applied to the 3D reconstruction of the histopathological structure of lung cancer, which is helpful to understand the spatial structure and distribution of various components of lung cancer lesions.

Unlike traditional sectioning followed by staining, in this study, staining is done before sectioning, which has the following advantages: 1) Convenient and time-saving staining procedure: The staining-then-sectioning method takes less time and is easier to operate than staining hundreds of slices after sectioning. 2) Uniform staining between adjacent sections: staining-then-sectioning method can better ensure uniform staining between adjacent sections than sectioning-then-staining, which facilitates image recognition after reconstruction. 3) Rapid and thorough dehydration without obvious decolorization. 4) One-step method of dehydration and transparency: isopropyl alcohol is used for both dehydration and transparency, which could further simplify the procedure and shorten the operation time. The HE staining method will be used in conjunction with the most fine-grained 3D imaging technique (fMOST) to construct 3D structural atlas data sets at single cell resolution level. The high-precision, repeatable, unbiased identification and classification of various types of cells can identify the pathological features and connection patterns of different subtypes of lung cancer, and provide a new technical approach for the study of the pathogenesis and development of lung cancer.

At the same time, there are several limitations of this method. Firstly, this study explored the en-bloc HE staining and consecutive sectioning of tissues with a size of about 1 cm × 1 cm × 0.3 cm, the staining and dehydration time for larger sized tissues may need to be further extended. Meanwhile, it is still a challenge to accomplish completely uniform staining of pure solid tumor, as the intermediate color is slightly light, but has no significant effect on the judgment of pathological features. Secondly, a variety of staining methods for various purposes can be performed on unstained paraffin sections produced using sectioning-then-staining method, while whether the HE-stained sections produced by staining-then-sectioning method can be rinsed for other staining methods needs to be explored in further study.

## Conclusion

In conclusion, a suitable en-bloc HE staining of centimeter-sized lung cancer and paracancerous tissues were identified with satisfactory results. It is promising to be applied to the 3D spatial assessment of the pathological features of lung cancer, which can help to accurately identify the sophisticated pathological features of lung cancer at 3D and single-cell level.

## Data availability statement

The original contributions presented in the study are included in the article/supplementary material, further inquiries can be directed to the corresponding author.

## Ethics statement

The studies involving human participants were reviewed and approved by Ethics Committee of Tianjin Chest Hospital (2022LW-024). The patients/participants provided their written informed consent to participate in this study.

## Author contributions

XLiu collected and selected the sample, MX performed the dehydration and embedding, DS and TL assessed and directed the procedure. XLi directed the work and guarantee the integrity of its results. YD and HW wrote the manuscript, which was reviewed by all authors.

## Funding

The research was funded by National Natural Science Foundation of Tianjin (No.21JCYBJC00260), Tianjin Key Medical Discipline (Thoracic Surgery) Construction Project (No. TJYXZDXK-018A), National Natural Science Foundation of China (No.81971660), Medical & Health Innovation Project (2021-I2M-1-042, 2021-I2M-1-058), Sichuan Science and Technology Program (No. 2021YFH0004), Tianjin Outstanding Youth Fund Project (No. 20JCJQC00230), Program of Chinese Institute for Brain Research in Beijing (2020-NKX-XM-14), and CAMS Innovation Fund for Medical Sciences (2022-I2M-C&T-B-001).

## Conflict of interest

The authors declare that the research was conducted in the absence of any commercial or financial relationships that could be construed as a potential conflict of interest.

## Publisher's note

All claims expressed in this article are solely those of the authors and do not necessarily represent those of their affiliated

organizations, or those of the publisher, the editors and the reviewers. Any product that may be evaluated in this article, or claim that may be made by its manufacturer, is not guaranteed or endorsed by the publisher.

## References

- Sung H, Ferlay J, Siegel RL, Laversanne M, Soerjomataram I, Jemal A, et al. Global cancer statistics 2020: GLOBOCAN estimates of incidence and mortality worldwide for 36 cancers in 185 countries. *CA Cancer J Clin* (2021) 71:209–49. doi:10.3322/caac.21660
- Nicholson AG, Tsao MS, Beasley MB, Borczuk AC, Brambilla E, Cooper WA, et al. The 2021 WHO classification of lung tumors: Impact of advances since 2015. *J Thorac Oncol* (2022) 17:362–87. doi:10.1016/j.jtho.2021.11.003
- Mäkinen JM, Laitakari K, Johnson S, Mäkitaro R, Bloigu R, Pääkkö P, et al. Histological features of malignancy correlate with growth patterns and patient outcome in lung adenocarcinoma. *Histopathology* (2017) 71:425–36. doi:10.1111/his.13236
- Thunnissen E, Beasley MB, Borczuk AC, Brambilla E, Chirieac LR, Dacic S, et al. Reproducibility of histopathological subtypes and invasion in pulmonary adenocarcinoma. An international interobserver study. *Mod Pathol* (2012) 25(12):1574–83. doi:10.1038/modpathol.2012.106
- Moreira AL, Ocampo PSS, Xia Y, Zhong H, Russell PA, Minami Y, et al. A grading system for invasive pulmonary adenocarcinoma: A proposal from the international association for the study of lung cancer pathology committee. *J Thorac Oncol* (2020) 15(10):1599–610. doi:10.1016/j.jtho.2020.06.001
- Yagi Y, Aly RG, Tabata K, Barlas A, Rektman N, Eguchi T, et al. Three-dimensional histologic, immunohistochemical, and multiplex immunofluorescence analyses of dynamic vessel co-option of spread through air spaces in lung adenocarcinoma. *J Thorac Oncol* (2020) 15:589–600. doi:10.1016/j.jtho.2019.12.112
- Kadota K, Kushida Y, Kagawa S, Ishikawa R, Ibuki E, Inoue K, et al. Cribriform subtype is an independent predictor of recurrence and survival after adjustment for the eighth Edition of TNM staging system in patients with resected lung adenocarcinoma. *J Thorac Oncol* (2019) 14:245–54. doi:10.1016/j.jtho.2018.09.028
- Onozato ML, Klepeis VE, Yagi Y, Mino-Kenudson M. A role of three-dimensional (3D) reconstruction in the classification of lung adenocarcinoma. *Stud Health Technol Inform* (2012) 179:250–6. doi:10.3233/978-1-61499-086-4-250
- Onozato ML, Kovach AE, Yeap BY, Morales-Oyarvide V, Klepeis VE, Tammireddy S, et al. Tumor islands in resected early-stage lung adenocarcinomas are associated with unique clinicopathologic and molecular characteristics and worse prognosis. *Am J Surg Pathol* (2013) 37:287–94. doi:10.1097/PAS.0b013e31826885fb
- Handschuh S, Schwaha T, Metscher BD. Showing their true colors: A practical approach to volume rendering from serial sections. *BMC Dev Biol* (2010) 10:41. doi:10.1186/1471-213X-10-41
- Streicher J, Weninger WJ, Müller GB. External marker-based automatic congruencing: A new method of 3D reconstruction from serial sections. *Anat Rec* (1997) 248:583–602. doi:10.1002/(SICI)1097-0185(199708)248:4<583:AID-AR10>3.0.CO;2-L
- Hine IF. Block staining of mammalian tissues with hematoxylin and eosin. *Stain Technol* (1981) 56:119–23. doi:10.3109/10520298109067294
- Li Y, Li N, Yu X, Huang K, Zheng T, Cheng X, et al. Hematoxylin and eosin staining of intact tissues via delipidation and ultrasound. *Sci Rep* (2018) 8:12259. doi:10.1038/s41598-018-30755-5
- Zheng T, Feng Z, Wang X, Jiang T, Jin R, Zhao P, et al. Review of micro-optical sectioning tomography (MOST): Technology and applications for whole-brain optical imaging [invited]. *Biomed Opt Express* (2019) 10:4075–96. doi:10.1364/BOE.10.004075
- Kato H, Oizumi H, Suzuki J, Hamada A, Watarai H, Sadahiro M. Thoracoscopic anatomical lung segmentectomy using 3D computed tomography simulation without tumour markings for nonpalpable and non-visualized small lung nodules. *Interact Cardiovasc Thorac Surg* (2017) 25:434–41. doi:10.1093/icvts/ivx113
- Ji Y, Zhang T, Yang L, Wang X, Qi L, Tan F, et al. The effectiveness of three-dimensional reconstruction in the localization of multiple nodules in lung specimens: A prospective cohort study. *Transl Lung Cancer Res* (2021) 10:1474–83. doi:10.21037/tlcr-21-202
- Maclean KS. Automatic and continuous staining with undiluted isopropyl alcohol as the sole dehydrant. *Stain Technol* (1962) 37:128. doi:10.3109/10520296209114591
- Viktorov IV, Proshin SS. Use of isopropyl alcohol in histological assays: Dehydration of tissue, embedding into paraffin, and processing of paraffin sections. *Bull Exp Biol Med* (2003) 136:105–6. doi:10.1023/a:1026017719668
- Koinzer S, Bajorat S, Hesse C, Caliebe A, Bever M, Brinkmann R, et al. Calibration of histological retina specimens after fixation in Margo's solution and paraffin embedding to *in-vivo* dimensions, using photography and optical coherence tomography. *Graefes Arch Clin Exp Ophthalmol* (2014) 252:145–53. doi:10.1007/s00417-013-2457-6
- Buesa RJ, Peshkov MV. Histology without xylene. *Ann Diagn Pathol* (2009) 13:246–56. doi:10.1016/j.anndiagpath.2008.12.005
- Leslie KO, Colby TV. Pathology of lung cancer. *Curr Opin Pulm Med* (1997) 3:252–6. doi:10.1097/00063198-199707000-00003
- Guo J, Meng S, Su H, Zhang B, Li T. Non-invasive optical monitoring of human lungs: Monte Carlo modeling of photon migration in Visible Chinese Human and an experimental test on a human. *Biomed Opt Express* (2022) 13:6389–6403. doi:10.1364/BOE.472530
- Meng S, Su H, Guo J, Wang L, Li T. Noninvasive optical monitoring of pulmonary embolism: a Monte Carlo study on visible Chinese human thoracic tissues. *J Biomed Opt* (2023) 28:015001. doi:10.1117/1.JBO.28.1.015001
- van Kuppevelt TH, Robbesom AA, Versteeg EM, Veerkamp JE, van Herwaarden CL, Dekhuijzen PN. Restoration by vacuum inflation of original alveolar dimensions in small human lung specimens. *Eur Respir J* (2000) 15:771–7. doi:10.1034/j.1399-3003.2000.15d23.x